Journal of Applied Mechanics and Technical Physics, Vol. 39, No. 5, 1998

EXPERIMENTAL INVESTIGATION OF PULSED STRETCHING OF CAVITATING MEDIA

S. V. Stebnovskii

UDC 532.135:532.52

A class of media whose structure develops into a foam state during pulsed volume stretching because of unrestricted growth of cavitational bubbles was determined experimentally. Among such media are low-viscosity Newtonian liquids, and disperse liquid media (emulsions, suspensions, and gels) with a low-viscosity liquid matrix. The results obtained are important for the development of a generalized rheological model for cavitating media.

To develop a generalized model for the failure of liquids that is valid in the range from low-viscosity ideal liquids to viscoelastic non-Newtonian liquids, it is necessary to have experimental information on the evolution of their structure under pulsed stretching conditions. The present paper reports results from an experimental study of the evolution of the structure of liquid media with different rheological properties stretched in a rarefaction wave.

1. A diagram of the setup used in the experiments is shown in Fig. 1. Here A is the gas gun used for pulsed loading of targets (samples of the liquids studied) by a piston impactor, B is the pulsed lighting with condensers, C is the camera (12 × 18 cm), and D is the measuring equipment. At the initial moment, receiver 1 is filled with air compressed to a given pressure $P_* = 3 \cdot 10^5$–$12 \cdot 10^5$ Pa. Thyratron-type valve 2 is closed, and electromagnetic valve 3 is open. Impactor piston 4 (a rigid foam plastic cylinder with a bonded "shock" plate made of Plexiglas) is located above valve 3 in the lower part of evacuated accelerating section 5. The liquid sample 9 being studied is positioned on easily destructible thin diaphragm 6 in chamber 7 with quadratic cross-sectional area (1.6 × 1.6 cm) and slit windows 8. The chamber is provided with damping device 10 to suppress the kinetic energy of the failing sample 9. After the valve 2 blows off, the piston is accelerated by the compressed air and the measuring equipment records its velocity when it arrives at optical transducers 12. Then, valve 3 closes, cutting off the air supply from the receiver to the accelerating section. The piston impacts the sample immediately after its velocity is recorded by the transducers. As a result, a shock wave with a triangle profile (shown on the right of Fig. 1) propagates in the media studied, and it is recorded by pressure gauge 11.

Axial stretching of the sample begins in the rarefaction stage after the shock front emerges on the free surface of the sample. The pressure behind the front of the shock wave generated in the sample is calculated from the measured velocity of the impactor and shock adiabats of the impactor and sample materials using the method of P, U diagrams. Thus, at $P_* = 3 \cdot 10^5$–$12 \cdot 10^5$ Pa, the velocity of an impactor of Plexiglas at the instant of impact varies in the range 68–200 m/sec, and the shock-front pressure in a water sample, for example, varies in the range $6 \cdot 10^7$–$22 \cdot 10^7$ Pa.

2. The following media were used as the samples:

(m1) water: a low-viscosity Newtonian liquid (shear viscosity $\mu = 1.003 \cdot 10^{-3}$ Pa · sec);

(m2) glycerin: a viscous Newtonian liquid ($\mu = 1.450$ Pa · sec);

Lavrent'ev Institute of Hydrodynamics, Siberian Division, Russian Academy of Sciences, Novosibirsk 630090. Translated from Prikladnaya Mekhanika i Tekhnicheskaya Fizika, Vol. 39, No. 5, pp. 122–125, September–October, 1998. Original article submitted January 28, 1997.

 0021-8944/98/3905-0758 $20.00

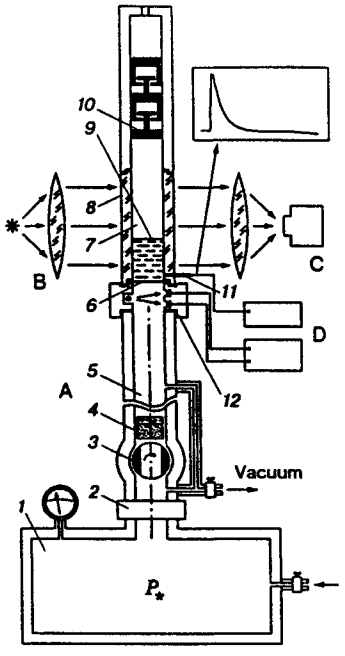

Fig. 1

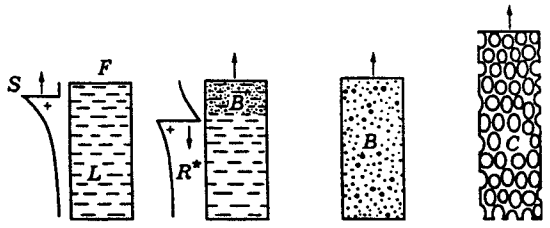

Fig. 2

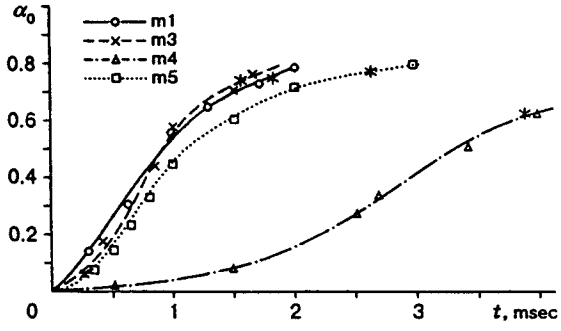

Fig. 3

(m3) an emulsion (a mixture of water and petrolatum drops of diameter $2 \cdot 10^{-4}$–$8 \cdot 10^{-4}$ cm with a volumetric concentration $\alpha_1 \approx 0.77$): a non-Newtonian pseudoplastic liquid having zero level of limiting shear stress ($\tau^* = 0$) and effective shear viscosity μ_* decreasing with increase in the shear stress rate $\dot{\varepsilon}$;

(m4) a lyophilic suspension (sand particles with sizes of $30 \cdot 10^{-4}$–$100 \cdot 10^{-4}$ cm and $\alpha_1 = 0.7$ in water): a dilatant non-Newtonian liquid with $\tau^* = 0$ and μ_* increasing with $\dot{\varepsilon}$;

(m5) gel (water, polyvinylpyrrolidone, propyleneglycol, and disodium salt of ethyleneditetraacetic acid): a solid-state Bingham body ($\tau^* > 0$) composed of a liquid matrix and ultradisperse solid particles forming structured systems, i.e., a thixotropic non-Newtonian liquid capable of restoring the structure after its mechanical failure at $\tau > \tau^*$ at which it enters a sol state.

Thus, using these samples, it is possible to perform a comparative analysis of the behavior of condensed media under pulsed volume stretching in the range of rheological parameters from a fluid low-viscous liquid to a solid-state Bingham body. In all experiments we used samples with dimensions 1.6 × 1.6 × 2.8 cm. A foam plastic float was placed on the free surface of a sample to prevent generation of jet flow (during stretching of the sample). The velocity and parameters of the impactor were chosen so that shock waves with a pressure at the front of the order of 10^8 Pa and length equal to the length of the sample were formed in all media.

3. The experiments performed showed the following. For all the media, cavitational bubbles begin to grow (zone B in Fig. 2) behind the front of the rarefaction wave R^* propagating in the sample L after emergence of the shock wave S on the free surface F. Figure 3 gives plots that illustrate the increase in the volume-averaged concentration of cavitational bubbles α_0 during the stretching process. The values of $\alpha_0(t)$ were determined from the increase in the volume of the stretched sample. It follows from the plots that the growth dynamics of α_0 practically does not depend on the rheological characteristics of the stretched liquid media but depends on their density. Indeed, media with similar densities but different rheological characteristics — m1 (low-viscosity water), m3 (highly concentrated emulsion), and m5 (solid-state gel after degradation of its structural viscosity in the rarefaction wave) have nearly equal rates of growth of cavitational bubbles. In medium m4 (a high-concentrated water–sand suspension), whose density is more than two times higher than the densities of media m1, m3, and m5, the growth rate α_0 is much lower.

Points that correspond to the stage of formation of cellular structures are denoted by asterisks on the plots (Fig. 2, zone C). Typical photographic records of cellular structures in media m1, m3, m4, and m5 are shown in Fig. 4a–d. It should be noted that the character of growth in α_0 is the same in all cases (Fig. 3)

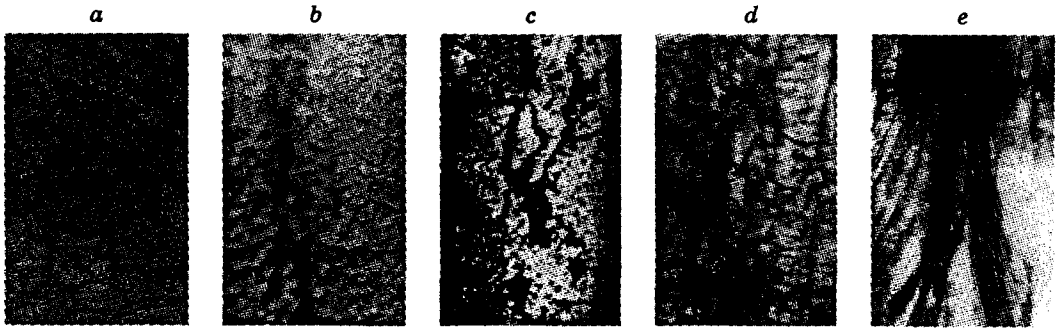

Fig. 4

but the cavitating media somewhat differ in structure. This is explained as follows. In medium m1, foam cells are formed in the homogeneous low-viscosity liquid matrix. Therefore, during growth, bubbles intensely coalesce and, hence, enlarge with the subsequent formation of a coarse-cellular foam medium. In m3, bubbles grow in the pseudoplastic emulsion matrix, and this makes coalescence of the bubbles rather difficult. As a result, the typical cell size is somewhat smaller than it is in the first case, but their number density is higher (for equal values of α_0). In the initial state, the thixotropic matrix of medium m5 contains micropores. In the volume stretching process, the structural viscosity of the medium decreases and the pores begin to grow because of the pressure difference. In this case, the low rate of coalescence is due to the residual structural viscosity of the gel, which enters a sol state in a vicinity of the pores. This results in a decrease in the typical cell sizes. In medium m4, the above effect becomes still more pronounced owing to the high density of the solid-disperse suspension matrix. Furthermore, in this case, the presence of coarse heavy lyophilic particles reduces the stability of the foam structure, and fragmentation of the medium begins earlier than it does in the first three cases (traces of the fragmentation are evident on the left of Fig. 4c).

Thus, although the structures of the media studied change differently during volume stretching because of the peculiarities of the cell's morphology, the process generally develops within the framework of a unified physical model, involving the stages of formation and unrestricted growth of cavitational bubbles or pores (in the case of m4), formation of cellular structures, and breakup of the medium into individual fragments.

As regards medium m2, its behavior is completely different. Behind the rarefaction-wave front in the medium, marked development of the cavitational process is not observed but dark stripes are formed which are reminiscent of a "fibrous" structure. Figure 4e gives a photograph of such a structure in a glycerin sample at a stretching stage that corresponds to the formation of cells in media m1, m3, m4, and m5 (Fig. 4a–d). It is obvious that in medium m2, cells are not formed because unrestricted development of cavitation does not occur in it. This is likely because of the too high dissipation energy due to the viscosity of the medium at the initial stage of development of cavitational bubbles, which "arrests" their further growth.

Indeed, the equation of bubble's dynamics for a viscous incompressible liquid [1] with allowance for surface tension σ,

$$R\ddot{R} + \frac{3}{2}\dot{R}^2 + (2\mu\dot{R} + \sigma)\frac{2}{\rho R} = \frac{P_1 - P_2}{\rho},$$

where R is the radius of a bubble, μ and ρ are the shear-viscosity coefficient and the liquid density, respectively, and P_1 and P_2 are the pressures in the bubble and the liquid, leads to the energy-balance equation

$$\frac{\rho}{2}R^3\dot{R}^2 = \frac{R^3 - R_0^3}{3}(P_1 - P_2) - (R^2 - R_0^2)\sigma - 4\mu\int_0^t R\dot{R}^2\,dt$$

at a moment t when the expanding bubble has radius R. Here the first term on the right is the specific work on expansion of the bubble from R_0 to R in counterpressure field P_2, the second term is the increase in the specific free energy of the system due to an increase in the bubble's surface from $4\pi R_0^2$ to $4\pi R^2$, and the third term is the energy dissipation caused by the liquid viscosity (per one steradian). Thus, in the case of

cavitational bubble growth in glycerin, the loss of energy due to dissipation is three orders of magnitude higher (other conditions being equal) than it is in the case of water. This significantly reduces the energy fraction expended on bubble expansion.

To establish the mechanism of formation of the "fibrous" structure during stretching in medium m2, it is necessary to perform an additional investigation.

Thus, the rheological model proposed previously [2, 3] for the development of the cavitational process and formation of cellular structures in stretched liquid media can be used to approximate the volume stretching of all low-viscosity homogeneous liquids and non-Newtonian liquids with a low-viscosity liquid matrix. The problem of modeling the structure of stretched high-viscosity liquids can be addressed after additional experimental studies of the development of bubble cavitation in these media and the hydrodynamic stability of their structure during volume stretching. This is also true for dispersed media with a high-viscosity liquid matrix.

This work was supported by the Russian Foundation for Fundamental Research (Grant No. 96-01-01772).

REFERENCES

1. H. Poritsky, "The collapse or growth of a spherical bubble or cavity in a viscous fluid," in: *Proc. First U.S. Nat. Congress Appl. Mech. (ASME)* (1952), pp. 813–821.
2. S. V. Stebnovskii, "On building a rheological model of cavitating dispersive liquid media," *Prikl. Mekh. Tekh. Fiz.*, **37**, No. 1, 109–117 (1996).
3. S. V. Stebnovskii, "Rheological model of volume stretching of Newtonian liquids," *Prikl. Mekh. Tekh. Fiz.*, **39**, No. 1, 30–39 (1998).